JOURNAL OF THEORETICAL
AND APPLIED MECHANICS
1, 38, 2000

GROUND RESONANCE OF A HELICOPTER

ZBIGNIEW DŻYGADŁO
GRZEGORZ KOWALECZKO

Military University of Technology, Warsaw

A method of the ground resonance phenomenon analysis is presented in this paper. It has been carried out for a one-main rotor helicopter on the basis of a complete set of nonlinear differential equations, known in flight mechanics. It has been modified by taking into account the forces and moments produced by a landing gear. Some results of numerical calculations for two models of landing gear-ground interactions are shown.

Key words: ground resonance, nonlinear helicopter dynamics

1. Introduction

A helicopter is a rotorcraft, which during its motion can be subjected, to various types of vibrations. For some of these vibrations there can appear self-excited oscillations caused by the interaction between the lagging motion of the rotor blades and other modes of the helicopter motion. The ground resonance is a specific case of vibrations, where the inertia forces react with the fuselage on its landing gear. These forces are caused by the out-of-phase lagging motion of particular blades. Frequency of inertia forces depends on the frequency of blades natural vibrations and on the angular velocity of the main rotor (Kuras and Żerek, 1966; Lytwin et al., 1970; Bramwell, 1976; Dymitruk and Żerek, 1984, 1985; Bojanowski, 1989; Szrajer, 1989; Ormison, 1991; Żerek, 1989). The out-of-phase lagging motion may be caused by blast of wind, damage of damper etc. The inertia forces cause oscillations of the fuselage on its landing gear. Oscillations of the fuselage produce a motion of the hub which, in turn, excites the lagging motion. The ground resonance occurs only in the case when the frequency of inertia forces and the fuselage frequencies are close to each other. For some values of the angular velocity of the main rotor, the interactions

between lagging motions of blades and motion of the fuselage are self-excited and they are responsible for unstable behaviour of the helicopters. The ground resonance was encountered soon after the introduction of helicopters. A lot of accidents were caused by this phenomenon.

In a classical theory of the ground resonance for a one-main rotor helicopter (Coleman and Feingold, 1958; Mil, 1967; Kuras and Żerek, 1966; Lytwin et al., 1970; Bramwell, 1976; Dymitruk and Żerek, 1984, 1985; Bojanowski, 1989; Szrajer, 1989; Ormison, 1991; Żerek, 1989; Szabelski, 1995) only the following motions are usually considered: lagging of the main rotor blades, rolling of the fuselage about the longitudinal axis Ox_k and displacement of its mass centre along the Oy_k axis. This resonance is called the lateral ground resonance. Sometimes the "longitudinal" resonance is also considered but it is not so important as the lateral ground resonance. On the assumption that the main rotor rotates in vacuum aerodynamic forces are not included into consideration. Many other simplifications assumed too.

In the present paper a nonlinear dynamic model of a helicopter is described. This model has been applied to investigation of the ground resonance phenomenon. A specific modelling of the one-main rotor helicopter has been implemented. "Specific" means that it has been adopted from flight mechanics. Usually it is applied to the analysis of flight mechanics problems, e.g., manoeuvres with stall aerodynamics effects or flight under conditions of the main rotor blade system failure. In this model no typical simplifications have been taken into account.

In the analysis it is assumed that the helicopter fuselage is a rigid body and the main rotor consists of four rigid blades which are considered separately. Each blade moves about its horizontal flapping hinge and vertical lagging hinge. The tail rotor has been treated as a hingeless and weightless source of thrust, which equilibrates the drag moment and ensures directional control of the helicopter. The latter is important when flight dynamics problems are considered.

Additionally, for analysing the ground resonance phenomenon, landing gear rigidity and damping have been taken into account.

2. Formulation of the problem

2.1. Systems of coordinates

To determine a mathematical model of the helicopter, the following systems

of coordinates are assumed: $Ox_gy_gz_g$ – earth-fixed moving coordinate system, $Ox_ky_kz_k$ – fuselage-fixed system, $Px''y''z''$ – system connected with an element of the main rotor hub with the origin at the centre of hub, $P_{Hi}x_i'y_i'z_i'$ – system connected with the flapping hinge P_{Hi} of the ith blade with the origin in this hinge, $P_{Vi}x_iy_iz_i$ – system connected with the ith blade of the main rotor with the origin in the lagging hinge P_{Vi} of the blade.

All these frames of reference are shown in Fig.1 and they are presented in details by Kowaleczko (1998).

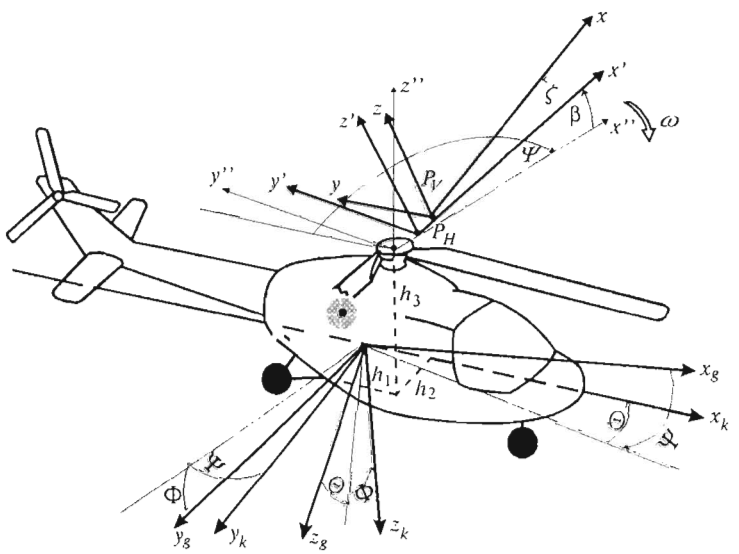

Fig. 1. Physical model of the helicopter and coordinate systems

The systems $Ox_gy_gz_g$ and $Ox_ky_kz_k$ are interconnected by the angles of yaw Ψ, pitch Θ and roll Φ.

The relation between them has the form

$$\boldsymbol{X}_k = \hat{\boldsymbol{\alpha}}\boldsymbol{X}_g \tag{2.1}$$

The elements of $\hat{\boldsymbol{\alpha}}$ matrix are

$$\hat{\boldsymbol{\alpha}} = \begin{bmatrix} \cos\Psi\cos\Theta & \sin\Psi\cos\Theta & -\sin\Psi \\ \cos\Psi\sin\Phi\sin\Theta - \sin\Psi\cos\Phi & \sin\Psi\sin\Phi\sin\Theta + \cos\Psi\cos\Phi & \sin\Phi\cos\Theta \\ \cos\Psi\cos\Phi\sin\Theta + \sin\Psi\sin\Phi & \sin\Psi\cos\Phi\sin\Theta - \cos\Psi\sin\Phi & \cos\Phi\cos\Theta \end{bmatrix}$$

The systems $Ox_ky_kz_k$ and $P_{Vi}x_iy_iz_i$, are interconnected by the angle Ψ_i, which is azimuth of the ith blade measured from the tail boom in the direction

of rotation of the main rotor, the angle β_i is flapping of the ith blade about the horizontal hinge and the angle ζ_i is lagging of the ith blade about the vertical hinge. This relation has the form

$$\boldsymbol{X} = \widehat{\gamma}_i \boldsymbol{X}_k \tag{2.2}$$

where $\widehat{\gamma}_i =$

$$= \begin{bmatrix} -\cos\psi_i \cos\beta_i \cos\zeta_i - \sin\psi_i \sin\zeta_i & -\sin\psi_i \cos\beta_i \cos\zeta_i + \cos\psi_i \sin\zeta_i & \sin\beta_i \cos\zeta_i \\ \cos\psi_i \cos\beta_i \sin\zeta_i - \sin\psi_i \cos\zeta_i & \sin\psi_i \cos\beta_i \sin\zeta_i + \cos\psi_i \cos\zeta_i & -\sin\beta_i \sin\zeta_i \\ -\cos\psi_i \sin\beta_i & -\sin\psi_i \sin\beta_i & -\cos\beta_i \end{bmatrix}$$

The analogous relation between $Ox_k y_k z_k$ and $P_{Hi} x_i' y_i' z_i'$ is

$$\boldsymbol{X}' = \widehat{\gamma}_i' \boldsymbol{X}_k \tag{2.3}$$

The matrix $\widehat{\gamma}_i'$ is obtained from the matrix $\widehat{\gamma}_i$ setting $\zeta_i = 0$.

The systems $Ox_k y_k z_k$ and $Px''y''z''$ are interconnected by the azimuth ψ. The relation has the form

$$\boldsymbol{X}'' = \widehat{\gamma}_i'' \boldsymbol{X}_k \tag{2.4}$$

The matrix $\widehat{\gamma}_i''$ is obtained from the matrix $\widehat{\gamma}_i$ setting $\zeta_i = 0$ and $\beta_i = 0$.

2.2. Determination of the equations of motion

The equations of motion have been derived on the basis of Newton's second law of dynamics. It has been applied separately to the fuselage, elements of each blade, elements of each connector and elements of the hub. On the basis of these equations the following equations have been obtained:

— Equations of translatory motion of the helicopter

$$M_k \frac{d\boldsymbol{V}_c}{dt} + \sum_{i=1}^{k} \int_{P_{Vi}}^{R} \boldsymbol{W}_i \, dm_i + \sum_{i=1}^{k} \int_{P_{Hi}}^{P_{Vi}} \boldsymbol{W}_i' \, dm_i' + \iiint_V \boldsymbol{W}'' \, dm'' = \boldsymbol{F} + \boldsymbol{T} + \boldsymbol{T}_{tr} \tag{2.5}$$

where

M_k	–	fuselage mass
$\boldsymbol{V}_c$	–	velocity of the centre of fuselage mass
$\boldsymbol{W}_i, \boldsymbol{W}_i', \boldsymbol{W}''$	–	absolute accelerations of the ith blade element, the ith connector element and the hub element, respectively
$\boldsymbol{F}$	–	vector of external forces acting on the fuselage
$\boldsymbol{T}_{tr}$	–	thrust of tail rotor
$\boldsymbol{T}$	–	vector of external forces acting on the rotor

$$\boldsymbol{T} = \sum_{i=1}^{k} \int_{P_{Vi}}^{BR} \boldsymbol{q}_i \, dr_i + \sum_{i=1}^{k} \int_{P_{Hi}}^{P_{Vi}} \boldsymbol{q}'_i \, dr'_i + \iiint_V d\boldsymbol{F}'' \tag{2.6}$$

B – tip-loss factor, $\boldsymbol{q}_i dr_i$, $\boldsymbol{q}'_i dr'_i$, $d\boldsymbol{F}''$ – vectors of external forces acting on ith blade element, on ith connector element and on hub element, respectively.

— Equation of equilibrium of moments about the centre of fuselage mass

$$\frac{d\boldsymbol{K}}{dt} + \sum_{i=1}^{k} \int_{P_{Vi}}^{R} \boldsymbol{R}_i \times \boldsymbol{W}_i \, dm_i + \sum_{i=1}^{k} \int_{P_{Hi}}^{P_{Vi}} \boldsymbol{R}'_i \times \boldsymbol{W}'_i \, dm'_i + \tag{2.7}$$

$$+ \iiint_V \boldsymbol{R}'' \times \boldsymbol{W}'' \, dm'' = \boldsymbol{M} + \boldsymbol{M}_T + \boldsymbol{M}_{tr}$$

where $\boldsymbol{R}_i$, $\boldsymbol{R}'_i$, $\boldsymbol{R}''$ are vectors which determine the locations of ith blade element, ith connector element and hub element relative to the centre of fuselage mass, respectively (Fig.2)

$$\boldsymbol{M}_T = \sum_{i=1}^{k} \int_{P_{Vi}}^{BR} \boldsymbol{R}_i \times \boldsymbol{q}_i \, dr_i + \sum_{i=1}^{k} \int_{P_{Hi}}^{P_{Vi}} \boldsymbol{R}'_i \times \boldsymbol{q}'_i \, dr'_i + \iiint_V \boldsymbol{R}'' \times d\boldsymbol{F}'' \tag{2.8}$$

is the moment of external forces about the centre of fuselage mass.

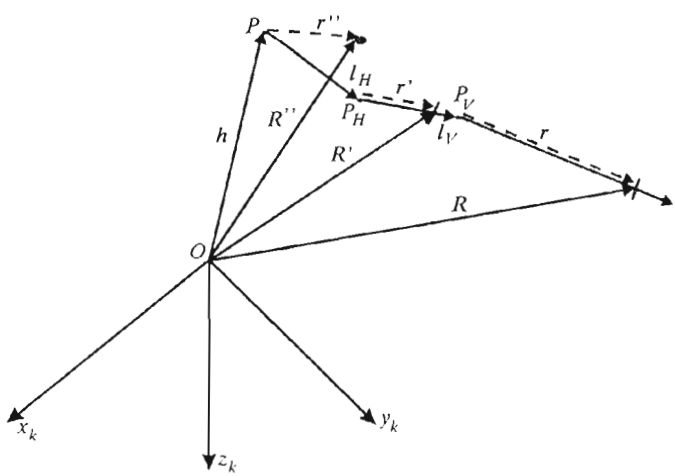

Fig. 2. Determination of blade, connector and hub element positions

— Equation describing the rotation of the main rotor around the axis of hub

$$\Big[\sum_{i=1}^{k}\int_{P_{Vi}}^{R}(\boldsymbol{l}_{Hi}+\boldsymbol{l}_{Vi}+\boldsymbol{r}_i)\times\boldsymbol{W}_i\,dm_i+\sum_{i=1}^{k}\int_{P_{Hi}}^{P_{Vi}}(\boldsymbol{l}_{Hi}+\boldsymbol{r}_i)\times\boldsymbol{W}_i'\,dm_i'\Big]_{z''}+$$
$$+\Big[\iiint_V \boldsymbol{r}''\times\boldsymbol{W}''\,dm''\Big]_{z''}=\Big[\boldsymbol{M}_P+\boldsymbol{M}_{rk}\Big]_{z''} \tag{2.9}$$

where $\boldsymbol{M}_{rk}$ is reaction moment of the fuselage which is under normal flow conditions equal to the moment of power system. $\boldsymbol{M}_P$ is moment of external forces about the hub centre $\boldsymbol{P}$. Its projection on Pz'' is determined by the relation

$$\begin{aligned}\Big[\boldsymbol{M}_P\Big]_{z''} &= \Big[\sum_{i=1}^{k}\int_{P_{Vi}}^{BR}(\boldsymbol{l}_{Hi}+\boldsymbol{l}_{Vi}+\boldsymbol{r}_i)\times\boldsymbol{q}_i\,dr_i\Big]_{z''}+\\ &+\Big[\sum_{i=1}^{k}\int_{P_{Hi}}^{P_{Vi}}(\boldsymbol{l}_{Hi}+\boldsymbol{r}_i)\times\boldsymbol{q}_i'\,dr_i'+\iiint_V \boldsymbol{r}''\times d\boldsymbol{F}''\Big]_{z''}\end{aligned} \tag{2.10}$$

— Equation of equilibrium of moments of forces acting on a blade about the flapping hinge P_H

$$\Big[\int_{P_{Vi}}^{R}(\boldsymbol{l}_{Vi}+\boldsymbol{r}_i)\times\boldsymbol{W}_i\,dm_i+\int_{P_{Hi}}^{P_{Vi}}\boldsymbol{r}_i'\times\boldsymbol{W}_i'\,dm_i'\Big]_{y_i'}=\Big[\boldsymbol{M}_{P_{Hi}}+\boldsymbol{M}_\beta\Big]_{y_i'} \tag{2.11}$$

The lower index $[\cdot]_{y_i'}$ indicates a projection on the axis $P_{Hi}y_i'$ of this hinge. $\Big[\boldsymbol{M}_{P_{Hi}}\Big]_{y_i'}$ is external moment acting on the blade about the axis $P_{Hi}y_i'$ of the hinge P_H

$$\Big[\boldsymbol{M}_{P_{Hi}}\Big]_{y_i'}=\Big[\int_{P_{Vi}}^{BR}(\boldsymbol{l}_{Vi}+\boldsymbol{r}_i)\times\boldsymbol{q}_i\,dr_i+\int_{P_{Hi}}^{P_{Vi}}\boldsymbol{r}_i'\times\boldsymbol{q}_i'\,dr_i'\Big]_{y_i'} \tag{2.12}$$

and $\Big[\boldsymbol{M}_\beta\Big]_{y_i'}$ is the sum of damping and spring moments of flap hinge $\Big[\boldsymbol{M}_\beta\Big]_{y_i'}=-c_\beta\dot{\beta}_i-k_\beta\beta_i$.

— Equation of equilibrium of the moments of forces acting on a blade about the lagging hinge P_V

$$\Big[\int_{P_{Vi}}^{R} \boldsymbol{r}_i \times \boldsymbol{W}_i \, dm_i\Big]_{z_i} = \Big[\boldsymbol{M}_{P_{Vi}} + \boldsymbol{M}_\zeta\Big]_{z_i} \tag{2.13}$$

The lower index $[\cdot]_{z_i}$ indicates a projection on the axis $P_{Vi}z_i$ of this hinge. $\Big[\boldsymbol{M}_{P_{Vi}}\Big]_{z_i}$ is the external moment acting on the blade about the axis $P_{Vi}z_i$ of the hinge P_V

$$\Big[\boldsymbol{M}_{P_{Vi}}\Big]_{z_i} = \Big[\int_{P_{Vi}}^{BR} \boldsymbol{r}_i \times \boldsymbol{q}_i \, dr_i\Big]_{z_i} \tag{2.14}$$

and $\Big[\boldsymbol{M}_\zeta\Big]_{z_i}$ is the sum of damping and spring moments of lagging hinge $\Big[\boldsymbol{M}_\zeta\Big]_{z_i} = -c_\zeta\dot{\zeta}_i - k_\zeta\zeta_i$.

These equations combined with kinematic relations

$$\dot{\Theta} = Q\cos\Phi - R\sin\Phi \qquad \dot{\Phi} = P + (Q\sin\Phi + R\cos\Phi)\tan\Theta$$
$$\dot{\Psi} = (Q\sin\Phi + R\cos\Phi)\frac{1}{\cos\Theta} \tag{2.15}$$

and

$$\frac{d\beta_i}{dt} = \dot{\beta}_i \qquad \frac{d\zeta_i}{dt} = \dot{\zeta}_i \tag{2.16}$$

have constituted the set of $18 + 2k$ nonlinear differential equations with periodic coefficients, where k is the number of blades of the main rotor. They can be expressed in the form

$$\mathbf{A}(t, \boldsymbol{X})\dot{\boldsymbol{X}} + \boldsymbol{B}(t, \boldsymbol{X}) = \boldsymbol{f}(t, \boldsymbol{X}, \boldsymbol{S}) \tag{2.17}$$

where $\boldsymbol{X}$ is the vector of flight parameters

$$\boldsymbol{X} = [U, V, W, P, Q, R, \omega, \dot{\beta}_i, \dot{\zeta}_i, \beta_i, \zeta_i, \psi, \Theta, \Phi, \Psi]^\top \qquad i = 1, ..., k$$

and

U, V, W – linear velocities of the centre of fuselage mass in the coordinate system $Ox_k y_k z_k$ fuselage fixed
P, Q, R – angular velocities of the fuselage in the same coordinate system
Θ, Φ, Ψ – pitch, roll and yaw angles of the fuselage, respectively
β_i – ith blade flapping rotation about the horizontal hinge P_H
ζ_i – ith blade lagging rotation about the vertical hinge P_V
ω – angular velocity of the main rotor
ψ – azimuth of the main rotor.

$\boldsymbol{S}$ is vector of control parameters

$$\boldsymbol{S} = [\theta_0, \kappa_s, \eta_s, \varphi_{s0}]^\top \qquad \text{or} \qquad \boldsymbol{S} = [\theta_0, \theta_1, \theta_2, \varphi_{tr}]^\top$$

where
θ_0 – angle of collective pitch of the main rotor
κ_s – control angle in the longitudinal motion
η_s – control angle in the lateral motion
φ_{tr} – angle of collective pitch of the tail rotor
θ_1, θ_2 – angles of cyclic pitches.

The detailed way of determining Eq (2.17) was presented by Kowaleczko (1998). For determination of matrix $\mathbf{A}$ and vector $\boldsymbol{B}$ there were established: locations of all helicopter elements, absolute velocities of these elements and their absolute accelerations.

For example for the ith blade element we have by turns (Kowaleczko, 1998):

— Location vector $\boldsymbol{R}_i$ (Fig.2)

$$\boldsymbol{R}_i = \boldsymbol{h} + \boldsymbol{l}_{Hi} + \boldsymbol{l}_{Vi} + \boldsymbol{r}_i \tag{2.18}$$

— Absolute velocity

$$\boldsymbol{V}_i = \boldsymbol{V}_c + \boldsymbol{V}_{\Omega i} + \boldsymbol{V}_{ri} \tag{2.19}$$

where
$\boldsymbol{V}_c$ – velocity of the centre of fuselage mass, $\boldsymbol{V}_c = [U, V, W]$
$\boldsymbol{V}_{\Omega i}$ – velocity resulting from the rotary motion of the fuselage, $\boldsymbol{V}_{\Omega i} = \boldsymbol{\Omega} \times \boldsymbol{R}_i$
$\boldsymbol{V}_{ri}$ – relative velocity produced by motions of blades about hinges and by the main rotor angular velocity $\boldsymbol{\omega}$,
$\boldsymbol{V}_{ri} = \boldsymbol{\omega} \times (\boldsymbol{l}_{Hi} + \boldsymbol{l}_{Vi} + \boldsymbol{r}_i) + \dot{\boldsymbol{\beta}}_i \times (\boldsymbol{l}_{Vi} + \boldsymbol{r}_i) + \dot{\boldsymbol{\zeta}}_i \times \boldsymbol{r}_i$.

— Absolute accelerations determined

$$\boldsymbol{W}_i = \frac{d\boldsymbol{V}_i}{dt} = \boldsymbol{W}_c + \boldsymbol{W}_{\varepsilon i} + \boldsymbol{W}_{\Omega i} + \boldsymbol{W}_{cor\,i} + \boldsymbol{W}_{ri} \tag{2.20}$$

where

$\boldsymbol{W}_c$ – absolute acceleration of the centre of fuselage mass, $\boldsymbol{W}_c = (\partial \boldsymbol{V}_c/\partial t) + \boldsymbol{\Omega} \times \boldsymbol{V}_c$

$\boldsymbol{W}_{\varepsilon i}$ – rotational acceleration, $\boldsymbol{W}_{\varepsilon i} = \boldsymbol{\varepsilon} \times \boldsymbol{R}_i$

$\boldsymbol{W}_{\Omega i}$ – centripetal acceleration, $\boldsymbol{W}_{\Omega i} = \boldsymbol{\Omega} \times (\boldsymbol{\Omega} \times \boldsymbol{R}_i)$

$\boldsymbol{W}_{cor\,i}$ – Coriolis acceleration, $\boldsymbol{W}_{cor\,i} = 2\boldsymbol{\Omega} \times \boldsymbol{V}_{ri}$

$\boldsymbol{W}_{ri}$ – relative acceleration, $\boldsymbol{W}_{ri} = (d\boldsymbol{V}_{ri}/dt) = (\partial \boldsymbol{V}_{ri}/\partial t) + (\boldsymbol{\omega} + \dot{\boldsymbol{\beta}}_i + \dot{\boldsymbol{\zeta}}_i) \times \boldsymbol{V}_{ri}$.

3. Forces and moments acting upon the helicopter

The vector $\boldsymbol{f}(t, \boldsymbol{X}, \boldsymbol{S})$ on the right-hand side of Eq (2.17) determines the external forces and moments acting on the helicopter and on its parts and represents also the right-hand sides of Eqs (2.15) and (2.16). These forces and moments may be divided into three groups: aerodynamic forces and moments; gravitation forces and moments; forces and moments produced by the landing gear. The aerodynamic and gravitation forces have the subscript a and g, respectively. The landing gear forces and moments have the subscript lg. We have

— Vector of external forces acting on the fuselage

$$\boldsymbol{F} = \boldsymbol{F}_a + \boldsymbol{F}_g + \boldsymbol{T}_{tr} + \boldsymbol{P}_{lg} \tag{3.1}$$

— Vector of external forces acting on the main rotor

$$\boldsymbol{T} = \boldsymbol{T}_a + \boldsymbol{T}_g \tag{3.2}$$

— Moment of external forces acting on the main rotor about the centre of fuselage mass

$$\boldsymbol{M}_T = \boldsymbol{M}_{Ta} + \boldsymbol{M}_{Tg} + \boldsymbol{M}_{lg} \tag{3.3}$$

— Moment of external forces acting on the fuselage

$$\boldsymbol{M} = \boldsymbol{M}_a + \boldsymbol{M}_g + \boldsymbol{M}_{tr} \tag{3.4}$$

— Eexternal moment acting on the blades about the axis Pz'' of shaft

$$\boldsymbol{M}_P = \boldsymbol{M}_{Pa} + \boldsymbol{M}_{Pg} \tag{3.5}$$

— External moment acting on the blade about the axis $P_{Hi}y_i''$ of hinge P_{Hi}

$$\boldsymbol{M}_{P_{Hi}} = \boldsymbol{M}_{P_{Hi}a} + \boldsymbol{M}_{P_{Hi}g} \tag{3.6}$$

— External moment acting on the blade about the axis $P_{Vi}z_i$ of hinge P_{Vi}

$$\boldsymbol{M}_{P_{Vi}} = \boldsymbol{M}_{P_{Vi}a} + \boldsymbol{M}_{P_{Vi}g} \tag{3.7}$$

According to (2.5) and (2.7), the forces and moments of the tail rotor have been shown. They have been indicated by subscript tr.

3.1. Mass forces and moments

The sum $\boldsymbol{F}_g + \boldsymbol{T}_g$ represents the resultant of gravitational forces acting on the helicopter. This vector is parallel to the axis Oz_g and has the magnitude $M_s g$. Making use of the matrix $\widehat{\boldsymbol{\alpha}}$, Eq (2.1), one can calculate components of this force in $Ox_k y_k z_k$.

The moment of mass forces acting on the fuselage about the centre of its mass is equal to zero

$$\boldsymbol{M}_g = \boldsymbol{0} \tag{3.8}$$

The moment of mass forces acting on the main rotor about the centre of fuselage mass is, according to Eq (2.8), equal to

$$\boldsymbol{M}_{Tg} = \sum_{i=1}^{k} \int_{P_{Vi}}^{BR} \boldsymbol{R}_i \times \boldsymbol{q}_{gi}\, dr_i + \sum_{i=1}^{k} \int_{P_{Hi}}^{P_{Vi}} \boldsymbol{R}_i' \times \boldsymbol{q}_{gi}'\, dr_i' + \iiint_V \boldsymbol{R}'' \times d\boldsymbol{F}_g'' \tag{3.9}$$

where $\boldsymbol{q}_{gi}dr_i$, $\boldsymbol{q}_{gi}'dr_i'$ and $d\boldsymbol{F}_g''$ are the vectors of elementary mass forces acting on the helicopter elements.

The moment of mass forces about the axis $P_{Hi}y_i'$ of ith flapping hinge is determined by the relation

$$\left[\boldsymbol{M}_{P_{Hi}g}\right]_{y_i'} = -g(l_V M_{bl} + S_{bl}\cos\zeta_i + S_r)\sum_{j=1}^{3} \gamma_{1j}'\alpha_{j3} \tag{3.10}$$

where

M_{bl} – mass of the main rotor blade
S_{bl} – static moment of the blade about the vertical hinge
S_r – static moment of the connector about the horizontal hinge.

The mass moment about the axis $P_{Vi}y_i$ of ith lagging hinge is equal to

$$\left[\boldsymbol{M}_{P_{Vi}g}\right]_{y_i} = -gS_{bl}\sum_{j=1}^{3} \gamma_{2j}\alpha_{j3} \tag{3.11}$$

3.2. Aerodynamic forces and moments

Aerodynamic forces and moments are generated by the main rotor and by the tail rotor and they also arise due to a flow around the fuselage and its elements. In the case of ground resonance all the aerodynamic forces produced by the flow around fuselage are neglected

$$\boldsymbol{F}_a = \boldsymbol{0} \qquad \boldsymbol{M}_a = \boldsymbol{0} \tag{3.12}$$

All the aerodynamic forces and moments produced by the main rotor have been obtained on the basis of Eqs (2.6), (2.8), (2.10), (2.12) and (2.14) making use of the blade element theory. Methodology of these calculations shown in detail in Kowaleczko (1998).

The aerodynamic load of the blade $\boldsymbol{q}_{ai}$ has the following components in the coordinate system $P_{Vi}x_iy_iz_i$

$$\boldsymbol{q}_{ai} = [0, q_{yai}, q_{zai}] \tag{3.13}$$

and the aerodynamic load of the connector has the following components in the coordinate system $P_{Hi}x_i'y_i'z_i'$

$$\boldsymbol{q}_{ai}' = [0, q_{yai}', q_{zai}'] \tag{3.14}$$

It has been assumed that the vector of aerodynamic forces acting on the hub is equal to zero $d\boldsymbol{F}_a'' = \boldsymbol{0}$.

3.3. Aerodynamic loads of the blade element

3.3.1. General form of formulae for aerodynamic loads

An elementary aerodynamic force $d\boldsymbol{R}$ (given per unit of the blade span) occurs as an effect of the flow around the blade elements. For further considerations only components of this force in the $P_{Vi}y_iz_i$ plane have been essential. In the coordinate system connected with the projection of local vector of the air velocity $\boldsymbol{V}$ on the $P_{Vi}y_iz_i$ plane the components of the force $d\boldsymbol{R}$ are

$$dP_{za} = C_{za}\frac{\rho V^2}{2}b(r) \qquad dP_{xa} = C_{xa}\frac{\rho V^2}{2}b(r) \tag{3.15}$$

where $b(r)$ is an aerodynamic chord of the blade airfoil.

However, the components of this force in the coordinate system $P_{Vi}x_iy_iz_i$ (see Fig.3), have been determined by the following relations

$$\begin{aligned} q_{zai} &= dP_{za}\cos\alpha^* + dP_{xa}\sin\alpha^* \\ q_{yai} &= dP_{xa}\cos\alpha^* - dP_{za}\sin\alpha^* \end{aligned} \tag{3.16}$$

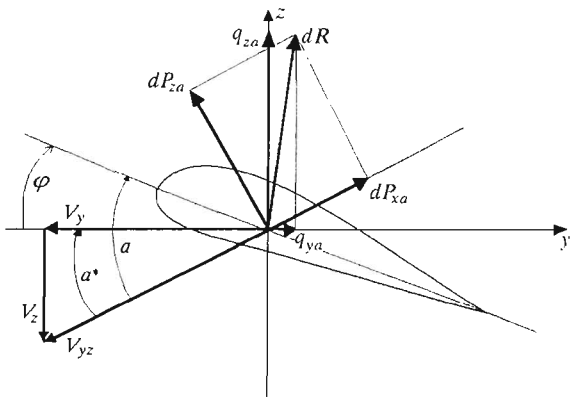

Fig. 3. Aerodynamic loads acting on the main rotor blade element

where α^* is the inflow angle. It is equal to

$$\alpha^* = \arctan \frac{V_z}{V_y} \tag{3.17}$$

The local vector $\boldsymbol{V}$ of the air stream flowing around the blade element is equal to the sum of absolute velocity $\boldsymbol{V}_i$ (2.19) and vector of induced velocity $\boldsymbol{v}_{ind}$. In the presented considerations it has been assumed that the induced velocity is a function of the blade radius and azimuth. This velocity, for each airfoil, has been determined by means of the Biot-Savart law – four separated strings of vortex have been investigated. The method of determining this velocity is not shown in this paper. For details the Reader is referred to Kowaleczko (1998).

According to the above considerations

$$\boldsymbol{V} = \boldsymbol{V}_i + \boldsymbol{v}_{ind}(\boldsymbol{l}_{Hi} + \boldsymbol{l}_{Vi} + \boldsymbol{r}_i, \psi_i) \tag{3.18}$$

V_y and V_z are the local velocity vector components.

The angle φ shown in Fig.3 is the blade pitch angle. It is determined by:
— Angle of collective pitch θ_0 of the main rotor, and cyclic angles θ_1 and θ_2 depending on the swash plate position
— Flapping angle β_i about the horizontal hinge (the effect of compensation of flapping determined by the compensation coefficient κ)
— Geometric torsion of blade

$$\varphi_r(r_i) = \theta_r r_i \tag{3.19}$$

Finally we have

$$\varphi = \theta_0 - \theta_1 \sin\psi_i - \theta_2 \cos\psi_i + \kappa\beta_i + \theta_r r_i \tag{3.20}$$

The aerodynamic coefficients used in Eqs (3.15) depend on the angle of attack of the blade airfoil and on the Mach number

$$C_{xa} = C_{xa}(\alpha, \mathrm{Ma}) \qquad C_{za} = C_{za}(\alpha, \mathrm{Ma}) \tag{3.21}$$

The angle of attack of the blade airfoil α (the section incidence), equal to (see Fig.3)

$$\alpha = \alpha^* + \varphi \tag{3.22}$$

The aerodynamic static characteristics of the NACA 23012 airfoil for Mach numbers from 0.3 to 0.8 for the full range of angles of attack have been assumed after Mil' (1967). They are shown in Fig.4 and Fig.5.

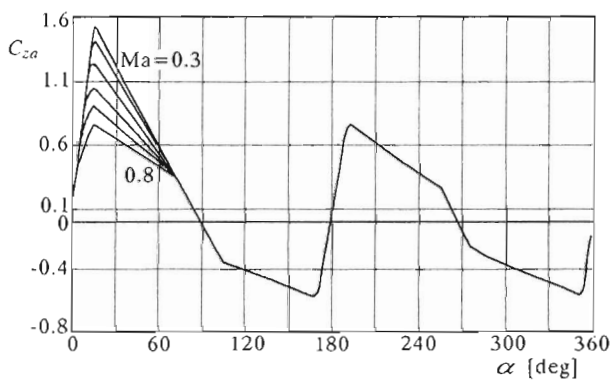

Fig. 4. Lift coefficient of the airfoil NACA 23012

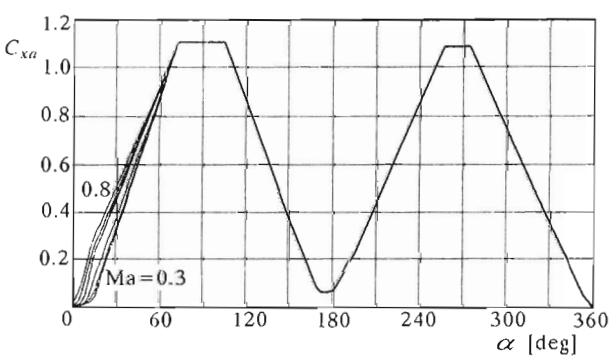

Fig. 5. Drag coefficient of the airfoil NACA 23012

3.3.2. Method of taking into account nonstationary effects

Specific flow conditions of the main rotor blades, even in a steady flight (motion about hinges, changeability of the air velocity flowing around airfoils depending on the blade azimuth, reverse flow region) cause that the section incidence α changes within a wide range. The critical angle of attack is often dynamically exceeded. This phenomenon is particularly visible for "retreating" blades near to the airscrew hub axis of rotation. The region within which the angle of stall is exceeded becomes larger when the speed of flight increases. Because of changes of the blade azimuth the sweep angle of the stream Λ changes also. This is a direct effect of the yawed component V_x of the airflow velocity $\boldsymbol{V}$ along the blade lengthwise axis. This component can be determined in the same way as the components V_y and V_z. One obtains

$$V_x = \gamma_{11i}(U + Qz_{ki} - Ry_{ki}) + \gamma_{12i}(V + Rx_{ki} - Pz_{ki}) + \\ +\gamma_{13i}(W + Py_{ki} - Qx_{ki}) - \omega(l_H + l_V \cos\beta_i)\sin\zeta_i + \left[\boldsymbol{v}_{ind}\right]_{x_i} \tag{3.23}$$

The sweep angle Λ is determined by the formula (see Fig.6)

$$\Lambda = \arctan\frac{V_x}{V_{yz}} \tag{3.24}$$

where $V_{yz} = \sqrt{V_y^2 + V_z^2}$.

According to the above description, it is necessary to include into consideration nonstationary aerodynamics for aerodynamic forces acting on blades to be determined correctly. The following way of calculating (according to Harris and Tarzanin, 1970; Tarzanin, 1971; Szumański, 1986; Kowaleczko, 1998) has been applied.

The initial data are: static angle of attack $\alpha_{st} = \alpha$ given by (3.17), Mach number Ma and reduced frequency determined as (Tarzanin, 1971)

$$k = \frac{b(r)\omega}{2V} = \frac{b(r)\omega}{2\sqrt{V_x^2 + V_y^2 + V_z^2}} \tag{3.25}$$

The static aerodynamic characteristics of the blade airfoil, which are shown in Fig.4 and Fig.5, are also applied. The scheme of further calculations is depicted in Fig.7.

The methodology of these calculations is as follows:

— The dynamic angle of attack of the airfoil is determined

$$\alpha_{dyn} = \alpha_{st} + \Delta\alpha_{dyn} = \alpha_{st} - k\sqrt{\left|\frac{\dot{\alpha}b(r)}{2V}\right|}\operatorname{sgn}\dot{\alpha} \tag{3.26}$$

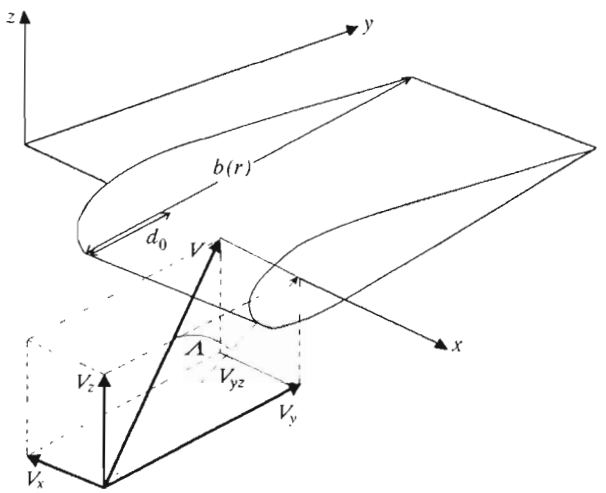

Fig. 6. Determination of the sweep angle Λ of the air stream flowing around the blade element

where k is an experimental constant of the airfoil.

— From the static lift characteristic one determines the value $C^*_{z_{st}} = C_{za}(\alpha_{dyn}, \mathrm{Ma})$. On the basis of this value tangent of a slope for the line drawn from the origin of coordinates to the point $(\alpha_{dyn}, C^*_{z_{st}})$ is calculated.

Simultaneously, the correction for the effect of the sweep Λ on the lift is taken into account

$$a_D = \frac{C^*_{z_{st}}}{\alpha_{dyn} \cos \Lambda} \tag{3.27}$$

— The equivalent angle of attack is calculated

$$\alpha_{eq} = \left[F(k)\alpha_{st} + \left(\frac{k}{2} + G(k)\right)\frac{d\alpha}{d\psi} + 2\left(\frac{3}{4} - \tilde{d}_0\right)F(k)k\frac{d\varphi}{d\psi} - k^2\left(\tilde{d}_0 - \frac{1}{2}\right)\frac{d^2\varphi}{d\psi^2}\right] \tag{3.28}$$

where

$F(k), G(k)$ – Theodorsen functions depending on the reduced frequency. These functions are shown in Fig.7. They are defined by means of Bessel functions

$\tilde{d}_0$ – relative location of the pitch axis (percent of chord aft of the leading edge), see Fig.6, $\tilde{d}_0 = d_0/b(r)$

φ – local pitch angle of blade element (3.20) depending on the azimuth ψ_i.

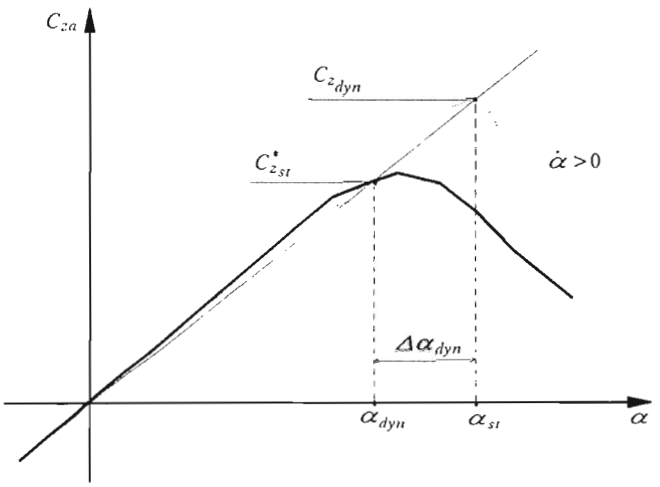

Fig. 7. Determination of the lift coefficient under dynamic stall conditions

— The lift and drag coefficients are calculated

$$C_z = \min\left\{a_D, \frac{dC_{z_{st}}}{d\alpha_{st}}\right\}\alpha_{eq} \qquad C_x = C_{xa}(\alpha_{dyn}, \mathrm{Ma}) \tag{3.29}$$

— The maximum value of coefficient C_z is limited and it satisfies the following relation

$$(C_z)_{\max} = \begin{cases} (C_{z_{st}})_{\max} + \left(3 - (C_{z_{st}})_{\max}\right)\dfrac{20\dot{\alpha}b(r)}{V} & \text{for } \left|\dfrac{\dot{\alpha}b(r)}{V}\right| < 0.05 \\ 3 & \text{for } \left|\dfrac{\dot{\alpha}b(r)}{V}\right| > 0.05 \end{cases} \tag{3.30}$$

where $(C_{z_{st}})_{\max}$ is the maximum value of the lift coefficient determined for a fixed Mach number with the use of static characteristic $C_{za}(\alpha, \mathrm{Ma})$.

In the course of calculations the following limitations have been considered:

- The above shown way of taking into account of nonstationary effects might be applied only in a limited range of angles of attack. This range is not clearly stated in the analysed papers. In the present paper the following limits have been assumed

$$-50^\circ < \alpha_{st} < 50^\circ \tag{3.31}$$

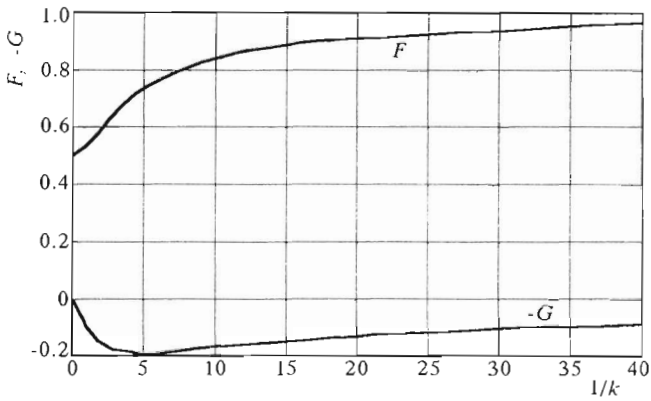

Fig. 8. Theodorsen functions versus $1/k$

- On the basis of analysed literature one can not determine the maximum value of the sweep angle Λ which gives correct value for expression (3.27). In the presented considerations this formula was employed for $|\Lambda| \leqslant 60°$. For higher absolute values of the sweep angles, the following relation was used

$$a_D = \frac{C^*_{z_{st}}}{\alpha_{dyn}} \tag{3.32}$$

- Under dynamic stall conditions the minimal value of coefficient C_z is not specified anywhere in the analysed literature for negative angles of attack. In this paper, likewise Eq (3.30), it was assumed that

$$(C_z)_{\min} = \begin{cases} (C_{z_{st}})_{\min} + \left(2 + (C_{z_{st}})_{\min}\right)\dfrac{20\dot{\alpha}b(r)}{V} & \text{for } \left|\dfrac{\dot{\alpha}b(r)}{V}\right| < 0.05 \\ -2 & \text{for } \left|\dfrac{\dot{\alpha}b(r)}{V}\right| > 0.05 \end{cases} \tag{3.33}$$

where $(C_{z_{st}})_{\min}$ is the minimal value of the lift coefficient for a specified Mach number determined from the static characteristic.

Examples of courses of the lift and drag coefficients, with dynamic stall effects taken into consideration, are presented in Fig.9 and Fig.10.

3.4. Landing gear forces and moments

When analysing the ground resonance it is necessary to take into account the forces and moments produced by a landing gear. It has been assumed

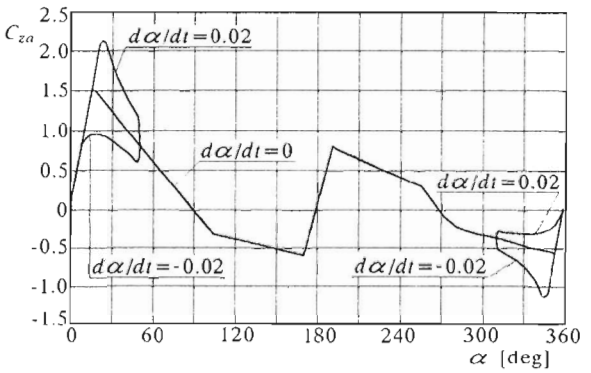

Fig. 9. Dynamic stall influence on $C_{za}(\alpha, \mathrm{Ma})$

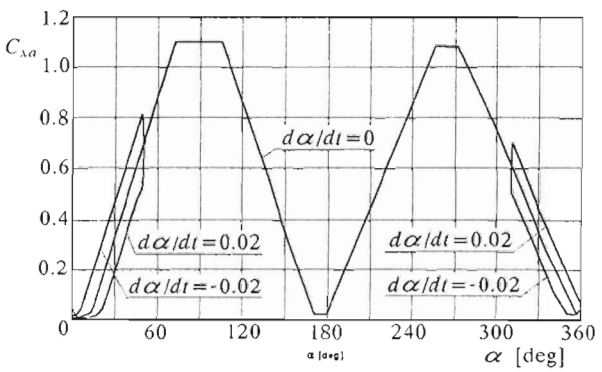

Fig. 10. Dynamic stall influence on $C_{xa}(\alpha, \mathrm{Ma})$

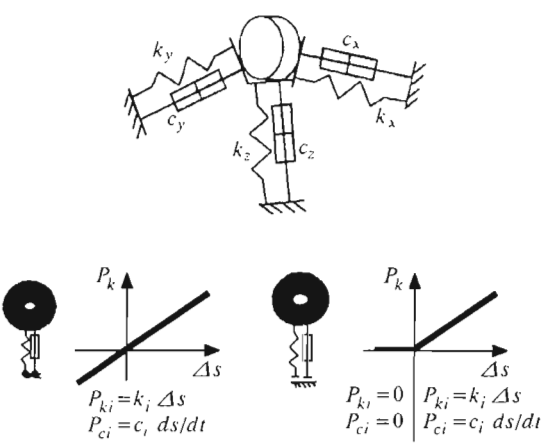

Fig. 11. Linear and nonlinear models of the landing gear

that the landing gear consists of three wheels. Configuration of the landing gear is shown in Fig.1. For each wheel its rigidity, damping and position have been determined separately. Two models of landing gear forces have been used (Fig.11). The first one, where relations between forces and displacement and velocity are linear

$$\boldsymbol{P}_{lg\,i} = \boldsymbol{P}_{ki} + \boldsymbol{P}_{ci} \tag{3.34}$$

and the second model where these relations are nonlinear – in the case where there is no contact between the wheel and ground. In this case all forces and moments produced by this wheel are equal to zero

$$\boldsymbol{P}_{lg\,i} = \begin{cases} \boldsymbol{P}_{ki} + \boldsymbol{P}_{ci} & \text{for} \quad \Delta h_i < 0 \\ 0 & \text{for} \quad \Delta h_i \geqslant 0 \end{cases} \tag{3.35}$$

where i is the number of wheel $(i = 1, 2, 3)$ and Δh_i is the distance between the wheel and the ground.

The components of the force $\boldsymbol{P}_{lg\,i}$ produced by the ith wheel are equal to

$$\begin{aligned} X_{lg\,i} &= -k_{xi}\Delta x_i - c_{xi}\dot{x}_i \\ Y_{lg\,i} &= -k_{yi}\Delta y_i - c_{yi}\dot{y}_i \\ Z_{lg\,i} &= -k_{zi}\Delta z_i - c_{zi}\dot{z}_i \end{aligned} \tag{3.36}$$

where

k_{xi}, k_{yi}, k_{zi} – stiffness coefficients of the ith wheel

c_{xi}, c_{yi}, c_{zi} – damping coefficients of the ith wheel

$\Delta x_i, \Delta y_i, \Delta z_i$ – displacements of the "contact point" determined in the system $Ox_k y_k z_k$.

The moment produced by the ith wheel is equal to

$$\boldsymbol{M}_{lg\,i} = \boldsymbol{R}_{lg\,i} \times \boldsymbol{P}_{lg\,i} \tag{3.37}$$

where the vector $\boldsymbol{R}_{lg\,i} = [x_{lg\,i}, y_{lg\,i}, z_{lg\,i}]$ determines the location of ith wheel relative to the centre of fuselage mass. The moment $M_{lg\,i}$ has the following components

$$\begin{aligned} L_{lg\,i} &= Z_{lg\,i} y_{lg\,i} - Y_{lg\,i} z_{lg\,i} \\ M_{lg\,i} &= X_{lg\,i} z_{lg\,i} - Z_{lg\,i} z_{lg\,i} \\ N_{lg\,i} &= Y_{lg\,i} x_{lg\,i} - X_{lg\,i} y_{lg\,i} \end{aligned} \tag{3.38}$$

Finally, the forces end moments produced by the landing gear are equal to

$$\begin{aligned} X_{lg} &= \sum_{i=1}^{3} X_{lg\,i} & Y_{lg} &= \sum_{i=1}^{3} Y_{lg\,i} & Z_{lg} &= \sum_{i=1}^{3} Z_{lg\,i} \\ L_{lg} &= \sum_{i=1}^{3} L_{lg\,i} & M_{lg} &= \sum_{i=1}^{3} M_{lg\,i} & N_{lg} &= \sum_{i=1}^{3} N_{lg\,i} \end{aligned} \tag{3.39}$$

3.5. Thrust of the tail rotor

As it has been stated at the beginning, the tail rotor is treated as the hingeless and weightless source of thrust which equilibrates the drag moment and ensures (in flight dynamics problems) directional control of the helicopter. According to this assumption, the thrust of the tail rotor has been calculated on the basis of the initial value of drag moment M_{P0} (Eq (2.16)). Making use of this value and the values of coordinates x_{tr} and z_{tr} ($y_{tr} = 0$), determining the location of the tail rotor relative to the centre of fuselage mass one obtains:

— Thrust of the tail rotor

$$T_{tr} = \frac{M_{P0}}{x_{tr}} \tag{3.40}$$

— Rolling and yawing moments produced by the tail rotor

$$L_{tr} = -T_{tr} z_{tr} \qquad N_{tr} = -T_{tr} x_{tr} \tag{3.41}$$

3.6. Final formulae for forces and moments

Summarising, the final formulae for the right-hand side of the set (2.17) (elements of vector $\boldsymbol{f}(t, \boldsymbol{X}, \boldsymbol{S})$) can be written in the following form

$$\begin{aligned} f_1 &= F_{x_k} = T_{ax_k} + X_g + X_{lg} \\ f_2 &= F_{y_k} = T_{ay_k} + Y_g + Y_{lg} + T_{tr} \\ f_3 &= F_{z_k} = T_{az_k} + Z_g \\ f_4 &= M_{x_k} = M_{Tax_k} + L_{Tg} + L_{lg} + L_{tr} \\ f_5 &= M_{y_k} = M_{Tay_k} + M_H + M_{Tg} + M_{lg} \\ f_6 &= N_{y_k} = M_{Taz_k} + N_{lg} + N_{tr} \\ f_7 &= \left[\boldsymbol{M}_{Pa} + \boldsymbol{M}_{Pg} + \boldsymbol{M}_{rk}\right]_{z''} \\ f_{7+i} &= \left[\boldsymbol{M}_{P_{Hi}a} + \boldsymbol{M}_{P_{Hi}g} + \boldsymbol{M}_{\beta}\right]_{y_i'} \end{aligned} \tag{3.42}$$

$$f_{7+k+i} = \left[\boldsymbol{M}_{P_{Vi}a} + \boldsymbol{M}_{P_{Vi}g} + \boldsymbol{M}_{\zeta}\right]_{z_i}$$

$$f_{7+2k+i} = \dot{\beta}_i \qquad f_{7+4k+1} = \omega$$

$$f_{7+3k+i} = \dot{\zeta}_i \qquad f_{7+4k+2} = Q\cos\Phi - R\sin\Phi$$

$$f_{7+4k+3} = P + (Q\sin\Phi + R\cos\Phi)\tan\Theta$$

$$f_{7+4k+4} = (Q\sin\Phi + R\cos\Phi)/\cos\Theta$$

Remark: In further analysis it is assumed that the angular velocity of the main rotor ω is constant. This assumption is reasonable if the angular velocity regulator is installed at the helicopter. It allows one to omit dynamics of engine. Also the seventh equation of the set (2.17) is neglected.

4. Solution to the problem

Eqs (2.17) have been applied to numerical simulations of the ground resonance phenomenon for the Polish "Sokol" helicopter. Some results of computation are presented in this paper. For all the cases presented, the initial position of the helicopter has been disturbed (particularly, the position of the second blade). The ground resonance is determined by the main rotor angular velocity, and therefore the angular velocity has been changed to study this phenomenon.

In the first set of figures (Fig.12) some selected parameters of the helicopter motion are shown. They have been determined for the nominal angular velocity ω_0 of the main rotor. One can see that all courses are damped. Of course, this means that helicopter is stable and no instability can occur. It is not important which model of the landing gear has been employed in numerical calculations. Because only the collective pitch of the main rotor θ_0 is not equal to zero, it is seen that damped oscillations of blades occur. Trajectory of the centre of fuselage mass moves to a stable point.

In Fig.13 the results of calculation of the ground resonance phenomenon are presented. It is known that the ground resonance consists of coupled motions: lagging of the main rotor blades, rolling of the fuselage and displacement of its mass centre along the lateral Oy_g axis. One can name this resonance as the lateral ground resonance. Sometimes the "longitudinal" resonance is also considered but it is not so important as the lateral ground resonance.

In the case presented in Fig.13 the linear model of landing gear has been applied. One can observe that all parameters increase but the values of pa-

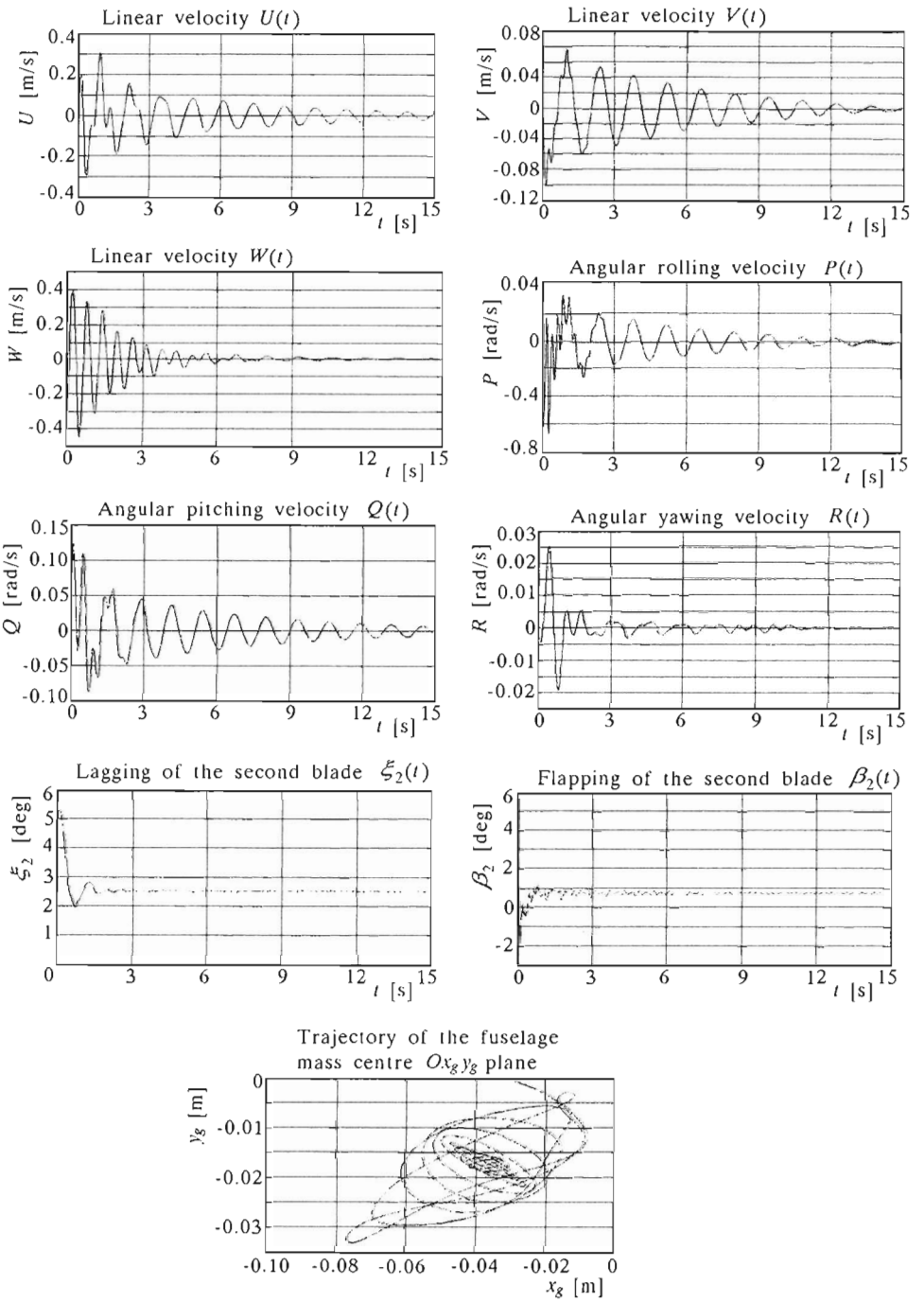

Fig. 12. Stable motions of the helicopter

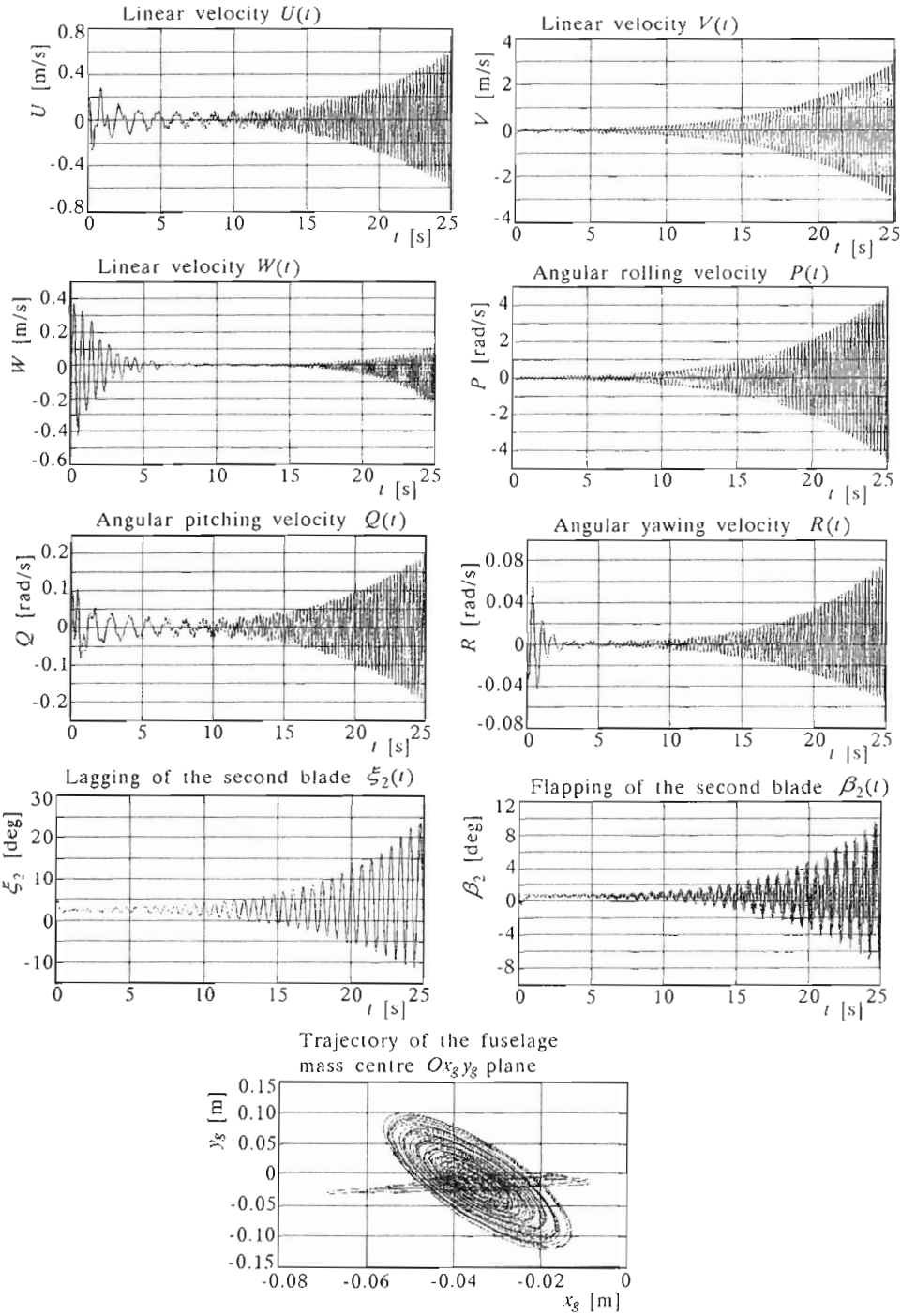

Fig. 13. Linear ground resonance of the helicopter

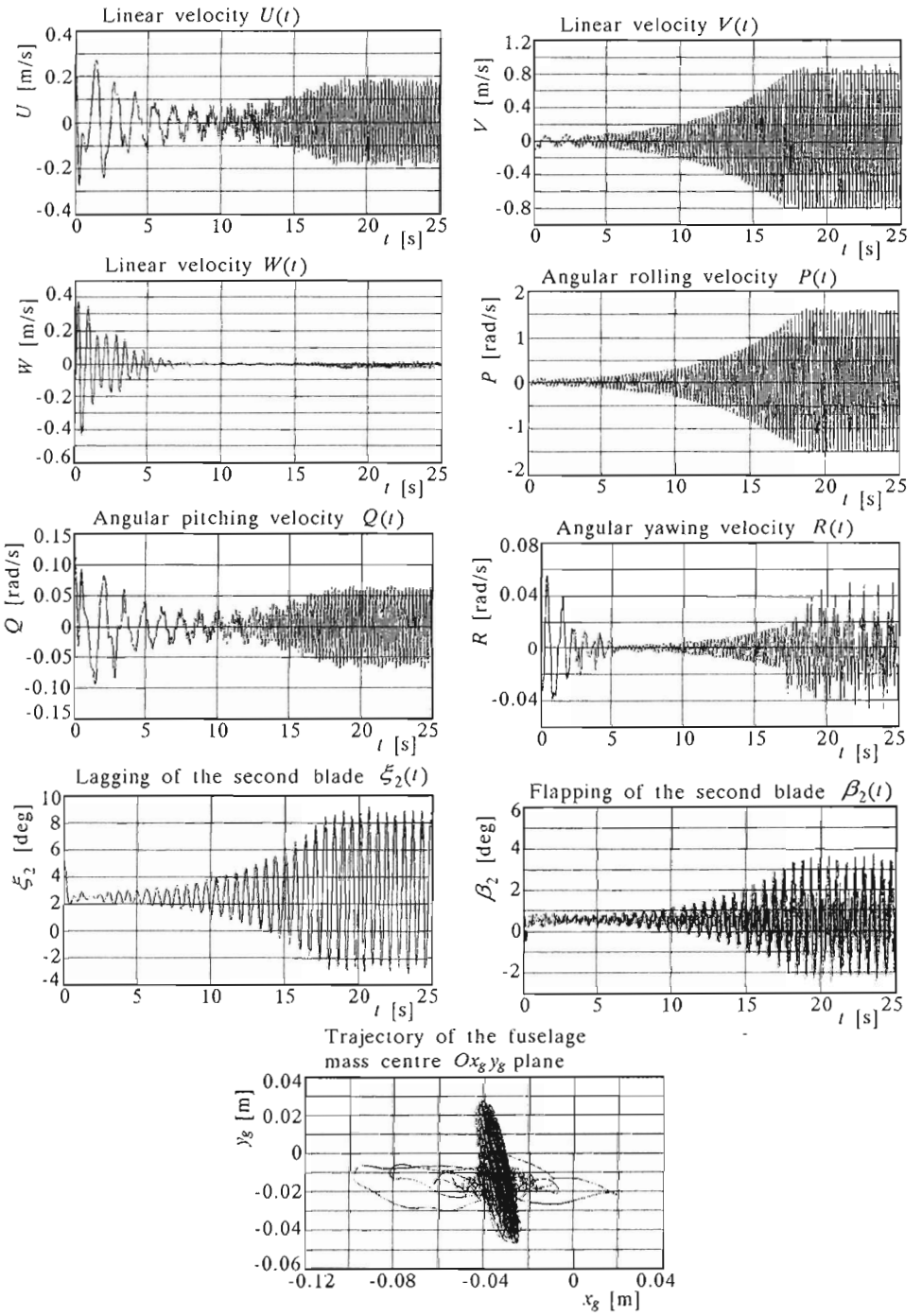

Fig. 14. Nonlinear ground resonance of the helicopter

rameters connected with lateral motions are greater than the parameters of describing longitudinal motion. Analysing motions of the second blade we can observe that the lagging angle oscillates with an increasing amplitude. This agrees with the classical theory of ground resonance. From the presented figures we can also see that the flapping angle of the blade is oscillating. Detailed analysis of this phenomenon allows us to draw a conclusion that this is due to cyclic changes of the Coriolis forces and aerodynamic forces acting on the blade. These forces change the flapping moment, which causes that the blade rotates around the flapping hinge.

Very interesting results have been obtained in the case of non-linear model of landing gear (Fig.14). In this instance the effects of nonlinearity are shown – at first oscillations are increasing and after that the amplitude of oscillations stabilises within a certain range. Detailed analysis shows that in this case the periods of oscillations increase. This takes place because average stiffness of the landing gear for one period decreases. It is presented in Fig.15.

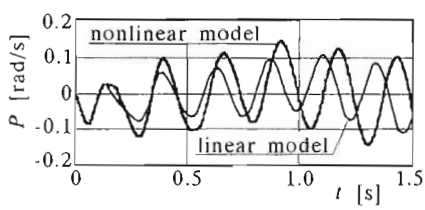

Fig. 15. Angular rolling velocity $P(t)$ – linear and nonlinear cases

If we make a comparison of the results of the classical theory of ground resonance with our results, it should be stated that the first theory, though very simplified, gives a correct physical picture of the ground resonance phenomenon.

In our model we could take into account a nonlinear dynamic model of a helicopter which enabled us to study a three dimensional ground resonance theory, where aerodynamic forces acting on lagging and flapping rotor blades have been taken into account together with linear or nonlinear landing gear models.

5. Concluding remarks

The paper presents the complete set of nonlinear differential equations which describes the ground resonance dynamics of the one-main rotor heli-

copter. This set has enabled us to study the helicopter fuselage motion and motions all the blades of the main rotor. Numerical analysis of the system dynamics has been performed and some results are given in the paper too. These results show time histories for various helicopter motion parameters. Basing on the obtained results we can conclude that the nonlinear model of the one-main rotor helicopter enables more precise study of physical phenomena which occur in reality. Making use of the presented model a further more detailed analysis of the ground resonance will be performed.

References

1. BOJANOWSKI J., 1989, Rezonans naziemny śmigłowca, *Prace Instytutu Lotnictwa*, **119**, Warszawa
2. BRAMWELL A., 1976, *Helicopter Dynamics*, Edward Arnold Publishers Ltd., London
3. COLEMAN R., FEINGOLD A., 1958, Theory of Self-Excited Mechanical Oscillations of Helicopter Rotors with Hinged Blades, NACA Report No. 1351
4. DYMITRUK D., ŻEREK L., 1984, Wpływ parametrów konstrukcyjnych smigłowca na jego rezonans przyziemny, *Prace Instytutu Lotnictwa*, **98**, Warszawa
5. DYMITRUK D., ŻEREK L., 1985, Rezonans przyziemny śmigłowca podczas rozbiegu, *Prace Instytutu Lotnictwa*, **102**, Warszawa
6. HARRIS F., TARZANIN F., 1970, Rotor High Speed Performance, Theory vs. Test, *Journal of the American Helicopter Society*, **15/32**
7. KOWALECZKO G., 1998, Nonlinear Dynamics of Spatial Motion of a Helicopter, Military University of Technology, Warsaw
8. KURAS R., ŻEREK L., 1966, Analiza rezonansu przyziemnego śmigłowców o zerowej podatności poprzecznej, *Prace Instytutu Lotnictwa*, **27**, Warszawa
9. LYTWIN R., MIAO W., WOITSCH W., 1970, Airborne and Ground Resonance of Hingeless Rotors, *26th Annual Forum of the American Helicopter Society*, Washington
10. MIL' M., 1967, *Vertolety. Raschet i proektirovane*, Izdatel'stvo Mashinostroene, Moskva
11. ORMISON R., 1991, Rotor-Fuselage Dynamics of Helicopter Air and Ground Resonance, *Journal of the American Helicopter Society*, **36**, 2
12. SZABELSKI K., 1995, *Wstęp do konstrukcji śmigłowców*, Wydawnictwa Komunikacji i Łączności, Warszawa

13. SZRAJER M., 1989, Badania symulacyjne rezonansu naziemnego, *Prace Instytutu Lotnictwa*, **119**, Warszawa

14. SZUMAŃSKI K., 1986, Transgresje układu pilot-śmigłowiec, Politechnika Warszawska

15. TARZANIN F., 1971, Prediction of Control Loads Due to Blade Stall, *The Annual National V/STOL Forum of the American Helicopter Society*, Washington

16. ŻEREK L., 1989, Rezonans naziemny śmigłowca z wirnikiem o doskonałej i przybliżonej symetrii z uwzględnieniem drgań łopat w płaszczyźnie ciągu, *Prace Instytutu Lotnictwa*, **119**, Warszawa

Naziemny rezonans śmigłowca

Streszczenie

W pracy przedstawiono metodę numerycznej analizy zjawiska rezonansu naziemnego. Analizę tą wykonano wykorzystując model matematyczny śmigłowca jednowirnikowego, w którym uwzględniono ruch poszczególnych łopat wirnika nośnego względem ich przegubów. Model ten został zaadoptowany z mechaniki lotu. Zmodyfikowano go wykorzystując do wyznaczenia sił i momentów od podwozia dwa modele: z uwzględnieniem oraz bez uwzględnienia odrywania się kół od podłoża.

Manuscript received Septemer 16, 1999; accepted for print October 6, 1999